ENVIRONMENTAL RESEARCH
LETTERS

LETTER • OPEN ACCESS

Assessing present and future coastal moderation of extreme heat in the Eastern United States

To cite this article: Colin Raymond and Justin S Mankin 2019 *Environ. Res. Lett.* **14** 114002

Environmental Research Letters

LETTER

Assessing present and future coastal moderation of extreme heat in the Eastern United States

Colin Raymond[1,2,5] and Justin S Mankin[3,4]

[1] Department of Earth and Environmental Sciences, Columbia University, New York, NY, United States of America
[2] Jet Propulsion Laboratory/California Institute of Technology, Pasadena, CA, United States of America
[3] Department of Geography and Department of Earth Sciences, Dartmouth College, Hanover, NH, United States of America
[4] Division of Ocean & Climate Physics, Lamont-Doherty Earth Observatory of Columbia University, Palisades, NY, United States of America
[5] Author to whom any correspondence should be addressed.

E-mail: cr2630@columbia.edu

Keywords: extreme heat, downscaled projections, coastal impacts, climate change, high resolution

Supplementary material for this article is available online

OPEN ACCESS

RECEIVED
4 July 2019

REVISED
20 September 2019

ACCEPTED FOR PUBLICATION
30 September 2019

PUBLISHED
22 October 2019

Abstract

Climate models suggest a rapid increase of extremely hot days in coming decades. Cool marine air currently ventilates extreme heat in populous coastal regions, diminishing its impacts, but how well climate models capture this effect is uncertain. Here we conduct a comprehensive observational analysis of coastal extreme-heat ventilation—its length scale, magnitude, and regional patterns—and evaluate two ensembles of downscaled global climate models along the eastern US coast. We find that coastal areas are 2 °C–4 °C cooler than ~60 km inland, resulting in reductions near 50% in population exposure to temperatures above 35 °C. Large seasonal and inter-regional variations are closely linked with land-sea temperature contrasts. High-resolution models underestimate coastal cooling by 50%–75%, implying that substantial and spatiotemporally varying model bias correction is necessary to create accurate projections of coastal extreme heat, which is expected to rise considerably with anthropogenic forcing. Our results underline the importance of regionally- and observationally-based perspectives for assessing future extreme heat and its impacts, and for positioning effective heat-risk management for communities and jurisdictions that span coast-to-inland areas.

1. Introduction

Extreme heat can have multiple and severe impacts in temperate and subtropical regions (Miller *et al* 2008, Dunne *et al* 2013, Horton *et al* 2016, Mora *et al* 2017). Fine-scale processes, such as local ocean-atmosphere or land-atmosphere interactions, often play a crucial role in climate extremes (Diffenbaugh *et al* 2005, Lebassi *et al* 2009). Such interactions prevail in coastal areas, which frequently experience warm-season daytime cooling. Well-defined sea breezes occur where the coast-to-inland temperature difference is large, but coastal cooling may be observed in the absence of a sea breeze as well (Lebassi-Habtezion *et al* 2011, Meir *et al* 2013).

Several previous studies have noted the importance of sea breezes and coastal moderation of extreme temperatures for ameliorating heat and pollution in coastal areas of Southern California (Clemesha *et al* 2018) and New York (Melecio-Vázquez *et al* 2018). Regional analyses have found important regional heterogeneity in projected future changes in these effects (Zhao *et al* 2011). However, no studies have focused directly on surveying coastal moderation of extreme high temperatures, nor how that influences population exposure. In addition, complex interacting atmospheric and marine processes make regional generalizations and comparisons difficult. Therefore, establishing a comprehensive and region-specific observational basis for coastal extreme-heat moderation is crucial for better understanding its spatial patterns and evaluating large projected increases in extreme heat (Gao *et al* 2012, Zobel *et al* 2017). Recent work on US temperature extremes has used global

Table 1. (Columns 1 and 2) The number of coastal grid points and regional hot days resulting from the PRISM analysis. The total number of points comprising each regional distribution is thus the product of these two columns. (Column 3) Summary of the means of the coastal-cooling intensity calculation discussed in the text. Intensity ranges span the 5th–95th percentiles of the distribution, making the cooling significant based on a two-tailed *t*-test.

Region	Coastal gridpts	Regional hot days	Mean intensity (°C)
Northern New England	95	561	4.52 (1.81–7.36)
New Jersey and Delmarva	49	529	2.69 (0.49–5.35)
Carolinas and Georgia	116	540	2.24 (0.31–4.44)
Florida Peninsula, Atl Coast	105	462	2.07 (0.35–4.04)
Florida Peninsula, Gulf Coast	59	484	1.88 (0.35–3.91)
Central Gulf Coast	182	458	2.42 (0.52–4.61)
Texas	104	404	3.69 (1.29–6.55)

climate models (GCMs) or reanalysis datasets that are too spatially coarse to resolve coast-to-inland temperature gradients and, consequently, the coastal-cooling phenomenon (Thibeault and Seth 2014, Wuebbles *et al* 2015, Ashfaq *et al* 2016, Papalexiou *et al* 2018); studies that do use high-resolution products typically take a broader view in their analysis (Gao *et al* 2012, Ning *et al* 2015, Zobel *et al* 2018). For those projections that rely on absolute temperature thresholds, bias corrections are necessary and often implemented, but there has been little analysis of how such corrections alter the picture of coastal exposure to extreme heat.

As heat extremes rapidly increase (Horton *et al* 2016), coastal moderation of extreme heat is paramount to understand and quantify, particularly its potential changes in a warming climate. This coastal moderation affects the heat exposure of about 50 million people in the eastern US alone, and nonlinear increases in health and economic impacts at the hottest temperatures make even small reductions meaningful (Wu *et al* 2014, Coffel *et al* 2018, Coffel *et al* 2019). Accurate assessment of the spatial footprint of future heat extremes is essential to local- and regional-scale efforts to manage heat exposure and its risks, as it enables financial, educational, medical, and other resources to be allocated according to need. For jurisdictions which include both coastal and inland communities, ongoing management of heat risks will necessarily need to be informed by the present magnitude of coastal cooling, as well as its future changes.

Here we conduct a systematic analysis of the extent to which historical heat extremes are moderated by marine influences in the eastern US, focusing on the 60 km wide coast-to-inland swath along the Atlantic and Gulf coasts. Using station and gridded observations, we analyze regional patterns of coastal cooling over the recent historical record to position our consideration of how projections of future heat extremes must be adjusted, due to the above-described model challenges, to reflect their true spatial distribution in coastal and near-coastal zones.

2. Methods

2.1. Observational data

We use historical daily-maximum temperature [T_{max}] data for 1981–2015 from the 4 km resolution parameter regression on independent slopes model (PRISM) (Daly *et al* 2008). PRISM takes station data as input and processes it using terrain- and coast-aware interpolations to produce a best-estimate gridded product (Daly *et al* 2003). In the eastern US PRISM employs a coastal-advection model that assumes a grid point's coastal influence is a function of distance from the coast, with bays and inlets treated as transition zones and terrain effects assumed negligible. Stations with similar coastal influence are weighted more heavily when computing grid point variables. Gridded 4 km resolution data is sufficient for capturing coastal cooling as observed from weather stations (Novak and Colle 2006, Lebassi-Habtezion *et al* 2011), a validation we also perform using the Global Surface Hourly and Global Historical Climatology Network-Daily datasets (Menne *et al* 2012). We conduct temperature-gradient and population-exposure analyses (see sections 2.4, 2.5) for seven regions (table 1, figure 1).

2.2. Model data

We employ data from two ensembles of daily-resolution downscaled GCMs (table S1 is available online at stacks.iop.org/ERL/14/114002/mmedia). From a dataset produced by Zobel *et al* (2017, 2018), we use an ensemble of five GCM model variants dynamically downscaled with the Weather Research and Forecasting (WRF) model to 0.1° (~11 km) resolution (hereafter referred to as the WRF ensemble). These data are for 1995–2004 (historical) and 2085–2094 (future, RCP8.5). From the localized constructed analogs (LOCA) project (Pierce *et al* 2014, 2015), we use a statistically-downscaled (~6 km resolution) ensemble of historical runs (1981–2005) and future projections for the high-emissions RCP8.5 scenario (2075–2099) for 14 GCMs (Meinshausen *et al* 2011). These 14 models are selected to span much of the range of the full CMIP5 suite while maintaining a variance that enables greater comparability with the WRF ensemble;

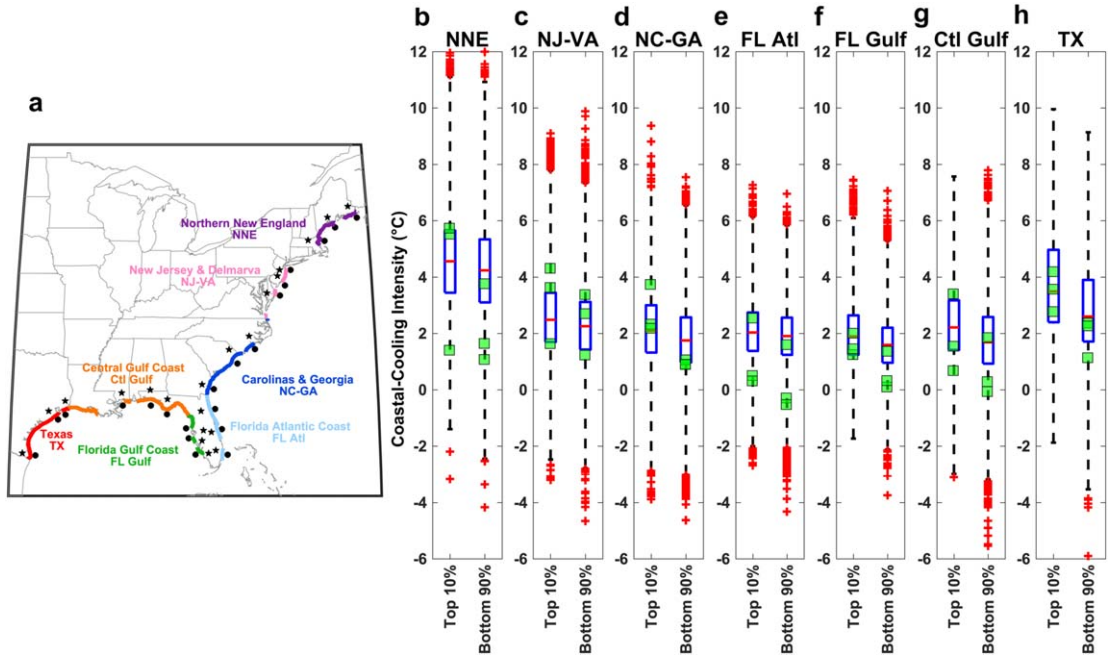

Figure 1. (a) Regions used in this study. Symbols indicate locations of inland (stars) and coastal (circles) stations used as verification for PRISM, with coastal stations offset for visibility. Heavy colored lines mark sections of coastline incorporated into the PRISM regional averages, as described in section 2.3. (b)–(h) Differences between inland and coastal daily maximum temperature in PRISM on regional hot days (left, top 10%) and all other days (right, bottom 90%). Green squares indicate the median of differences between the three inland-coastal station pairs for each region.

however, other model choices may produce slightly different results.

2.3. Defining coastal and inland areas

To ensure accurate comparison among gridded products, we match grid points based on their region and distance from the model-defined coastline, rather than by their absolute geographical location. We focus our analysis on coastline sections where coastal weather stations face the open ocean and that do not have bays or estuaries larger than 50 km in width, as these can introduce complex weather patterns that could confound the coastal cooling effects we seek to identify (Novak and Colle 2006). Terrain-complexity concerns also motivate our focus on the eastern US, where terrain variations are small within 100 km of the coast. For each section of coastline we define an 'inland' area located 60 km away, perpendicular to the local coastline direction. This 60 km distance is far enough inland to be beyond the reach of daytime coastal effects (Finkele 1998, Hu and Xue 2016), and small enough that differences due to synoptic-scale weather conditions are minimized.

2.4. Defining hot days and coastal cooling

We focus on characterizing coast-to-inland temperature differences rather than attempting to attribute such differences to driving processes, such as sea breezes, clouds, or precipitation. We define hot days as the top decile of daily T_{max} in the warm season (defined as May–September), based on a daily grid point climatology temporally smoothed with a Gaussian filter—a common method for avoiding spurious day-to-day variations (Freychet *et al* 2018). For each region, 'regional hot days' are then defined as those for which >50% of regional inland grid points are experiencing a hot day, following Smith *et al* (2013).

We calculate the 'coast-to-inland temperature difference' on a regional hot day as the difference between daily T_{max} along the coast (averaged over each set of three adjacent coastal grid points within that region) and daily T_{max} 60 km inland (averaged over each set of three corresponding inland grid points). We define the magnitude of coastal cooling for each regional hot day as being *proportional* to this coast-to-inland temperature difference. We choose to quantify the coastal-cooling magnitude in this way because temperature does not always steadily increase moving inland (figure S1). Instead, the temperature gradient can be nonmonotonic. To this end, we define 'coastal-cooling intensity' as equal to 75% of the coast-to-inland temperature difference (figure S1). Selecting a percentage higher (lower) than 75% results in a larger (smaller) value of coastal-cooling intensity, but does not affect the regions relative to one another according to our sensitivity analysis (figure S2). Averaging over many grid points and hot days (table 1) allows for statistically robust conclusions.

2.5. Populations and avoided exposure

We estimate coastal populations using the 1 km resolution Gridded Population of the World dataset

(CIESIN 2016); our estimate of 50 million people within 60 km of the Atlantic and Gulf coasts aligns well with previous reports (Wilson and Fischetti 2010). To assess the benefits of coastal cooling, we estimate the avoided exposure to extreme heat due to coastal cooling. We calculate avoided exposure by assuming that T_{max} at 60 km inland represents a counterfactual case for the coast—that is, what coastal temperatures would have been if not for coastal-cooling effects—and take its difference from the actual coastal temperature. We multiply this difference by the grid point population and define it as the avoided population-weighted extreme-heat exposure.

To assess the effect of model bias on projected extreme-heat exposure in coastal regions, we calculate two cases of population exposure to daily maximum temperatures >35 °C. The first case is a best estimate where we bias-correct the WRF and LOCA projections with PRISM observations by adding the model-derived 21st-century changes to the PRISM climatology. In the second case, the model projections are not bias-corrected. For both cases, we decompose the future changes in population exposure into two components: the contribution from changes in mean temperatures, and the contribution from changes in the coast-to-inland temperature gradient. We do this by generating an additional coast-to-inland temperature profile with the historical gradient but the future mean temperature. The mean-change contribution is obtained by comparing the historical temperature profile with this artificial one, while the gradient-change contribution is estimated by comparing the artificial profile with the future profile. In all cases, we assume that populations are fixed in size and spatial distribution.

3. Results

3.1. Characterization of observations

High-resolution, spatially complete PRISM data reveals that coastal daily-maximum temperatures are suppressed by several degrees Celsius relative to nearby inland areas (figure 1), in agreement with previous studies over more limited domains in the eastern US (Meir *et al* 2013, Melecio-Vázquez *et al* 2018). These coastal-cooling intensities differ considerably across regions—median values range from around 2 °C for the Southeast US to near 3.5 °C for Texas and 4 °C for Northern New England (figure 1). Within each region, large temporal variability in coastal-cooling intensity exists; however, each region's interquartile range is only 1 °C–2 °C, allowing for the differences between the largest and smallest coastal-cooling-intensity regions to be statistically significant at the 95% level.

A positive land-sea temperature contrast exists in all regions during summer, and in both seasonal and regional terms, it is closely associated with the coastal-cooling intensity (figure 2). This finding is consistent with the land-sea contrast being a known driver of ephemeral sea breezes (Lebassi-Habtezion *et al* 2011, Sequera *et al* 2015). The coastal-cooling effects we identify are consistently present on nearly all hot days (figure 1), however, underscoring their importance in reducing extreme-heat exposure.

Comparing the distributions of PRISM and GHCN-station-derived coastal-cooling intensities using quantile-quantile plots, we find PRISM exhibits biases for days with coastal cooling greater than 10 °C and also for coastal warming (figure S3). These appear to be related to PRISM's data interpolation, manifested particularly in a poor representation of days with fast-changing synoptic conditions and large coast-inland temperature differences. (We consider differences between PRISM and stations in more detail in the Discussion.) However, PRISM biases are less than about 1 °C–1.5 °C for coastal-cooling values in the 0 °C–5 °C range, which comprise the majority of hot days—ensuring the validity of our subsequent analyses and conclusions for these days.

Together, these results emphasize three important aspects of observed extreme heat in coastal areas. Firstly, for the majority of days, PRISM gridded climatology captures the cooling magnitudes from more-targeted station data, suggesting that PRISM is an appropriate observational basis against which to evaluate downscaled models (figure 1); secondly, the coastal-cooling phenomenon is present on nearly all warm-season days and across regions (figure 1); and thirdly, the magnitude of observed warm-season coastal cooling is highly regionalized, in part because it is closely associated with the magnitude of regional land-sea contrasts (figures 1, 2).

3.2. Evaluation of downscaled GCMs

Compared to PRISM, the LOCA and WRF downscaled products ubiquitously underestimate observed coastal cooling: their typical mean cooling is 0.5 °C–2 °C, at least a factor of two (and up to a factor of 10) smaller than observed (figure 3). These model biases in the coast-to-inland temperature gradient are large, and consist of two primary types (figures S4, S5): a mean temperature bias at each grid point and a temperature-gradient bias concerning the difference between coastal and inland grid points (figure 3). Over the historical period, LOCA's mean coast-to-inland temperature gradient is no more than about 1 °C (figure 3), suggesting that statistical downscaling does not sufficiently correct for the inability of the coarser parent model to represent the fine-scale coastal processes governing this gradient. Additionally, the LOCA methodology depends on using land-based stations to form analogs (Pierce *et al* 2014). As these stations are located on land, and few are near the coast, the LOCA reference points are tied to locations with little marine influence. This separation between the majority of LOCA stations and the coast makes the downscaling

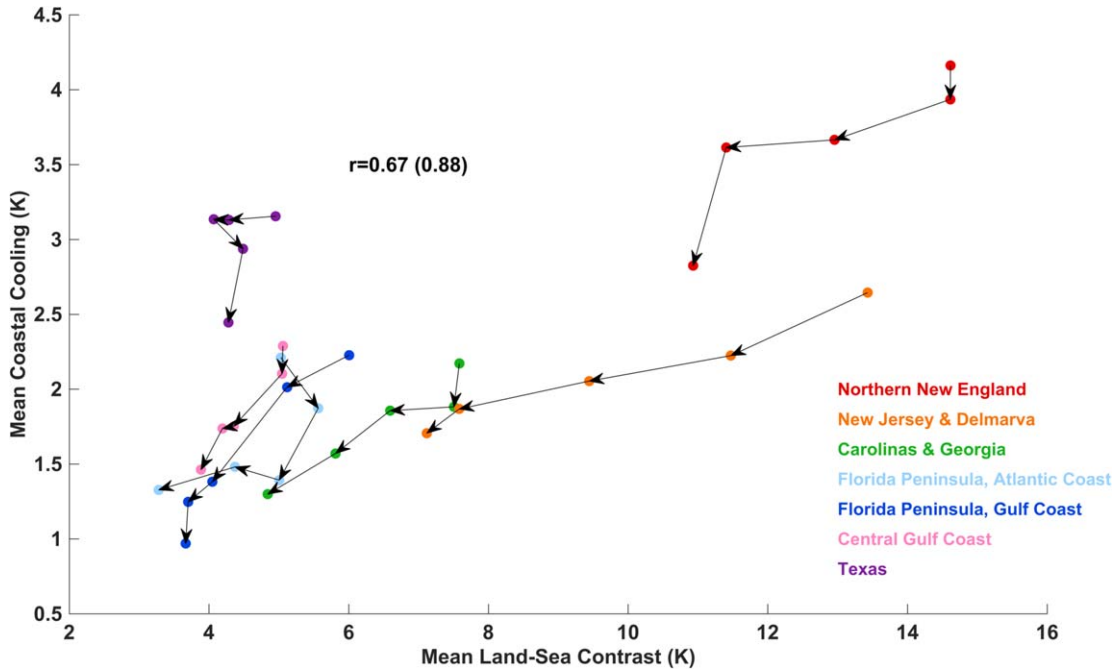

Figure 2. Correlation between mean land-sea contrast on regional hot days (ordinate) and mean corresponding coastal cooling (abscissa). Colors represent regions, for which the seasonal evolution of monthly averages from May to September is indicated by the arrows. As noted in the text, the correlation across all regions and months is 0.67, or 0.88 excluding Texas.

procedure less likely to capture the coastal-cooling effects we explore here despite its improved resolution.

Close to the coast, the dynamically-downscaled WRF ensemble performs somewhat better, reproducing the majority of the modest coastal-cooling effect for the Gulf Coast regions (figures 3(e)–(g)), but missing the large cooling magnitudes in other regions (figures 3(a)–(d)). The WRF ensemble is more skillful than LOCA for the Texas coast-to-inland temperature gradient, perhaps a function of WRF representing coastal atmospheric processes that are absent from the coarser global models that are the basis for the LOCA downscaling. Both products remain at a resolution where their ability to represent fine-scale coastal cooling is likely muted relative to observations (see Discussion).

The two ensembles point to a greater future increase in extreme heat at inland locations relative to the coast, amounting to a modest (~0.5 °C) strengthening of the coastal-cooling effect across all regions (figure 3). Even with such coastal-cooling increases, only the WRF future projections approach the magnitude of coastal cooling present in the historical observations, and only for the southernmost regions.

3.3. Population exposure

To understand how coastal cooling (and its model representation) influences future extreme-heat impacts assessments, we consider how models and observations vary in their estimated human exposure to extreme heat. Observationally, we find that, compared to the counterfactual case where temperatures in the coastal swath are identical to those 60 km inland, coastal cooling reduces present-day eastern-US population-weighted exposure to temperatures above 35 °C by more than half for locations within 20 km of the coast (figure S6). The greatest reductions occur closest to the coast and for the highest temperatures—for example, 40 °C almost never occurs anywhere along the immediate coast. Over the entire 60 km coastal swath and all regions considered, observed annual exposure to 35 °C heat is about 200 million person-days, or 4 d per person, versus 7 d per person in the counterfactual case, consistent with other findings (Jones *et al* 2015).

If we bias-correct the LOCA and WRF ensembles with PRISM observations to provide a best estimate of future changes in coastal extreme heat, population exposure to 35 °C extreme heat nearly triples by 2100 under a high-emissions scenario, to ~650 million person-days (figure 4(a)). The models also project an intensification of the coast-to-inland temperature gradient (figure 3), which could serve to partially counter the increased population exposure projected from mean temperature changes. As such, we decompose the change in population exposure to extreme heat into two components: one due to the mean warming across the 60 km coastal swath, and one due to the change in the temperature gradient within that swath. We find that the effects of mean warming dominate, with the model-projected increase in coastal cooling having a comparatively small effect (figure 4(a)).

Due to their mean bias and relatively weak temperature gradients, models effectively systematically understate the magnitude of coastal cooling, thereby

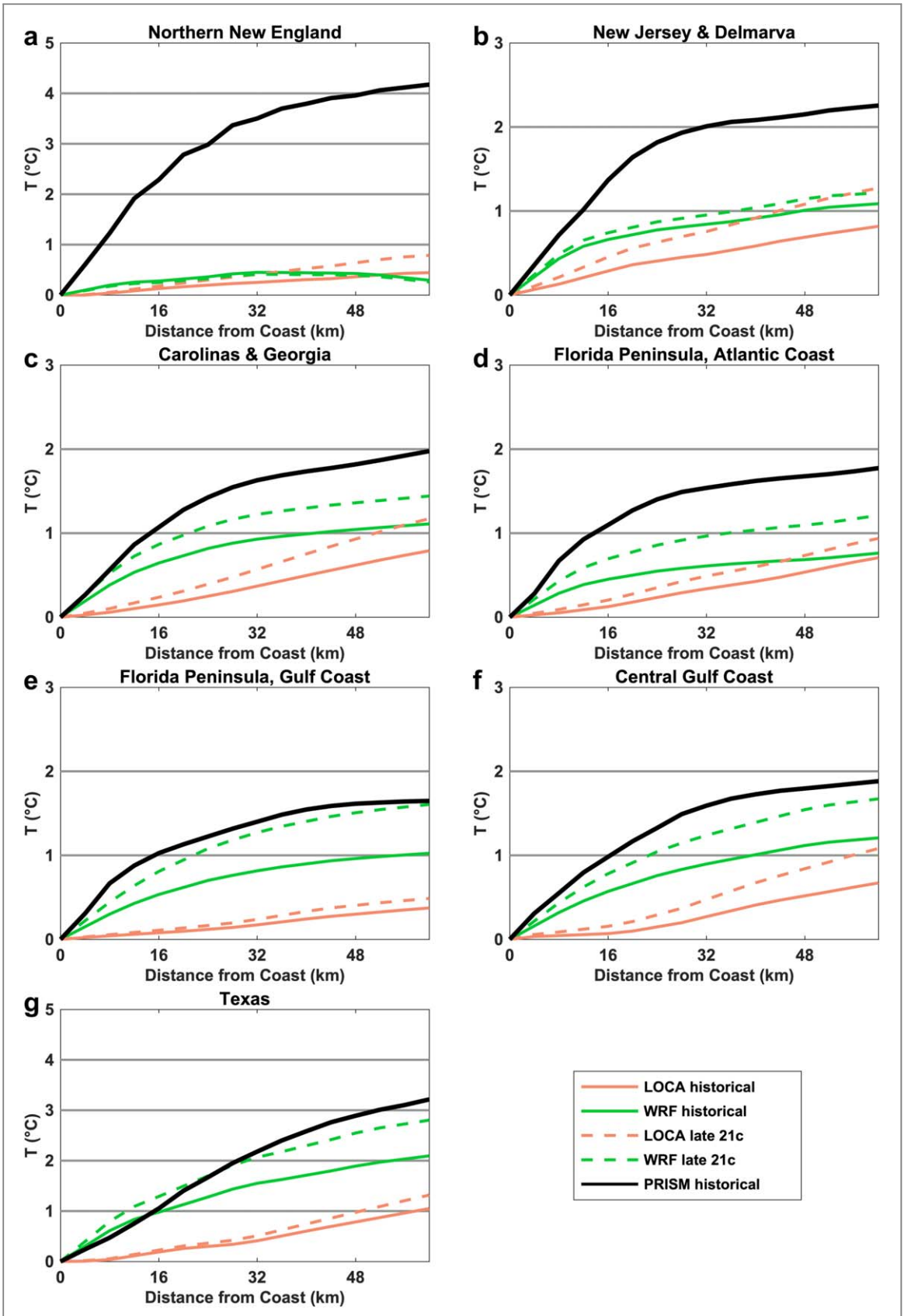

Figure 3. Mean maximum temperatures within the 60 km coastal swath on regional hot days, expressed relative to the coastal temperature as represented by each product. For the historical period, we plot data only for the overlapping period of record, 1995–2004: 4 km PRISM (black), 6 km LOCA (solid orange), and ~11 km WRF (solid green). Future projections under the RCP8.5 emissions scenario for 2075–2099 are dashed.

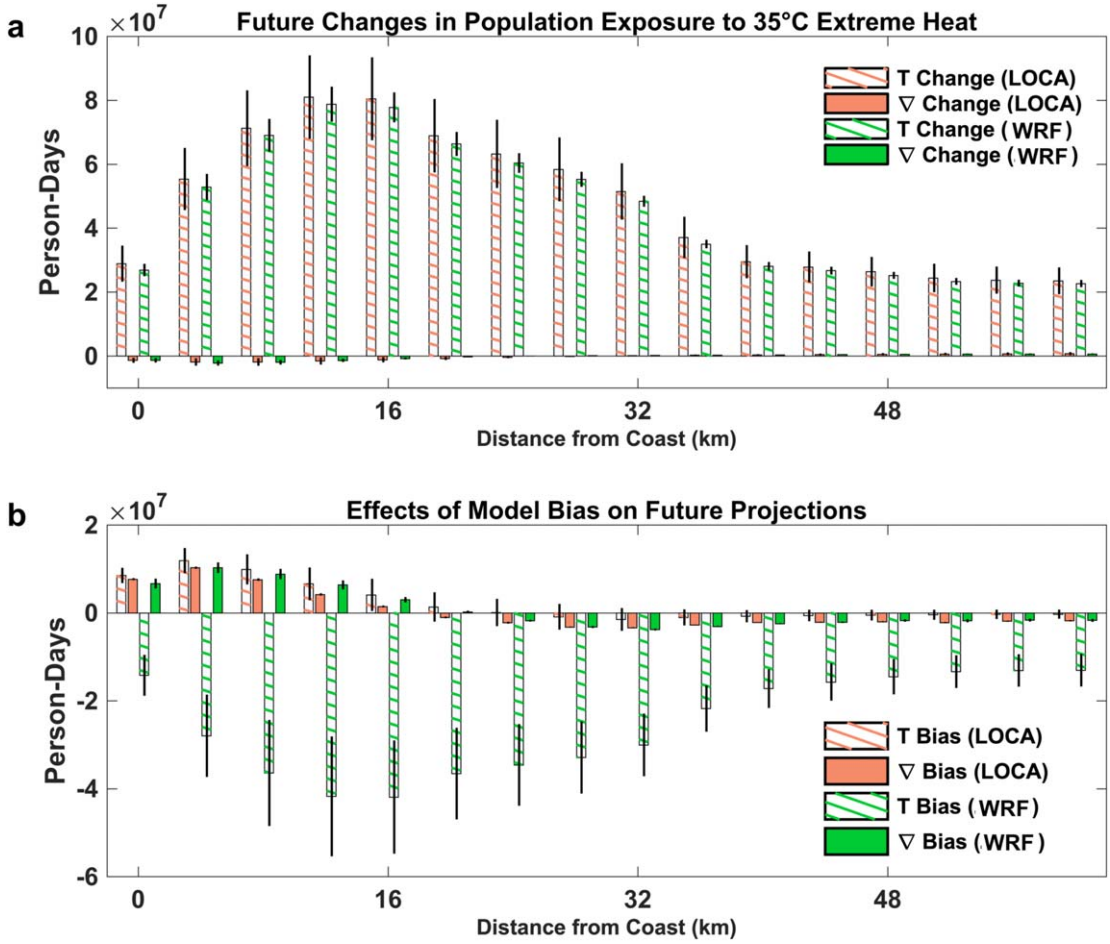

Figure 4. (a) Contributions of changes in mean temperature (hatched) and in coast-to-inland-temperature-gradient steepness (solid shading) to future population exposure to extreme heat in the LOCA (orange) and WRF (green) ensembles. Changes are calculated using bias-corrected values to allow for meaningful comparability. Error bars indicate a cross-model uncertainty of ± one standard deviation from the mean. (b) As in (a) but for contributions from model biases affecting the population-exposure projections. The sum of (a) and (b) returns the nonbias-corrected projections of the two ensembles.

overestimating coastal extreme heat (figure 3). We next investigate the characteristics of the bias correction that it is necessary to implement in order for models' future coastal extreme-heat risk estimates to be accurate. We recalculate population extreme-heat exposure, without bias-correcting the LOCA and WRF ensembles. We decompose the effects of the two different sources of model bias—the mean change (T bias) and the gradient bias (∇ bias)—on estimated population exposure (figure 4(b)). This decomposition makes clear that, in both ensembles, a weak coast-to-inland temperature gradient causes up to a 15% overestimate of late-21st-century population exposure to extreme heat within 16 km of the coast, though these effects become smaller further inland (solid bars in figure 4(b)). Mean-temperature biases (hatched bars) vary from moderately positive to strongly negative, the latter being about 50% of the projected changes. Members within each ensemble generally agree well, as indicated by the cross-model standard deviations.

4. Discussion and conclusions

The consistency of the coastal cooling that we observe across most warm-season days, in all regions (figure 1), leads us to propose that sea breezes are only part of a larger set of phenomena that determine the magnitude and inland extent of coastal cooling. Morning fog, midday clouds, a weak and ill-defined sea breeze, or a shallow coastal inversion layer are some of the alternative possibilities for propagation mechanisms, although investigating their contributions will require significant future research to determine how they may vary by region, season, or time of day. We find that latitudinal differences in mean cooling intensity are well-correlated with regional and seasonal land-sea temperature contrasts ($r = 0.67$) (figure 2); as the land-sea contrast decreases over the summer, so does the associated cooling effect. This correlation rises to 0.88 when Texas is excluded, indicating that it exhibits a markedly different behavior, which we propose to explain by noting that the Texas coast experiences strong low-level onshore flow due to the North Atlantic subtropical high during summer (Liang *et al*

2006, Hu and Xue 2016). Prior results have also described deep inland infiltration of marine air under persistent onshore-flow conditions (Arritt 1993, Gilliam *et al* 2004, Misra *et al* 2011).

As some of the only high-resolution multi-decadal simulations spanning the entire eastern US, the LOCA and WRF ensembles have a spatial comprehensiveness that enables estimation of the degree to which downscaled products overstate coastal extreme heat in both current and future climates. Our analysis suggests that this overstatement is considerable (several degrees Celsius), particularly for the large observed temperature gradients within 10–20 km of the coast in New England (figure 3), meaning that heat-exposure analyses using high-resolution downscaled ensembles nonetheless require observationally based bias correction to avoid major biases in heat exposure. For coarser-scale model output, bias correction is even more important; our results contextualize and evaluate this correction, which is implemented as a common remedy for their insufficient representation of coastal temperature gradients.

While a significant part of the downscaled products' bias is likely attributable to their coarser spatial resolution relative to PRISM, several pieces of evidence suggest the importance of additional factors. Firstly, the LOCA and WRF ensembles (6 km and ∼11 km resolution, respectively) are more similar to each other than to 4 km PRISM; secondly, their biases vary substantially between regions; and thirdly, the WRF ensemble generally exhibits less bias than LOCA despite its coarser spatial resolution. Such large and pervasive model biases are observed in other US coastal areas (Lebassi *et al* 2009, Wang and Kotamarthi 2014), though often varying considerably by region.

Therefore, an essential question that this study raises concerns the origin of the model biases that we have identified for the coast-to-inland temperature gradients. The accuracy of these gradients is crucial for assessing the magnitude and location of present and future extreme heat exposure, and thus for climate risk management (Kunreuther *et al* 2013). Statistically downscaled products, such as the LOCA ensemble, are sensitive to GCM physics and weather-station boundary conditions, whereas dynamically downscaled products, such as the WRF ensemble, are sensitive to high-resolution model physics and GCM boundary conditions. Our investigation suggests that dynamical downscaling may be better suited to capture coastal cooling, given the importance of sub-grid-scale, sub-daily dynamics. Nevertheless, statistical downscaling that incorporates sufficient marine observations could also strongly aid in reducing the persistent biases of dynamical models, whatever their resolution. Quantifying the biases associated with each strategy, and their variation according to location, season, and synoptic-scale meteorological pattern, is critical for making further progress in extreme-heat projections, especially because the choice of downscaling method is the single largest source of uncertainty for high-resolution climate projections (Li *et al* 2012, Xie *et al* 2015, Zhang and Soden 2019). This likely would encompass studying the parameterizations of sub-grid-scale processes in each GCM and in regional models such as WRF.

However, the modest intermodel spread in coastal cooling (figures S7, S8) suggests that selecting parent models on the basis of skill in representing important physical processes—the strategy proposed by Maraun *et al* (2017)—presents only a partial solution, as it is the downscaling method itself that generates a significant portion of the uncertainty. What is most evident from our analysis is that careful, regionalized bias correction is essential prior to evaluating coastal moderation of extreme heat. Such analysis greatly improves confidence in model projections, and is consistent with the practice of retaining the signal associated with model products (Hall 2014).

It should not be overlooked that PRISM also has certain biases and uncertainties relative to station data, reported here as well as in the dataset description (Daly *et al* 2008). These biases derive from the incomplete spatial coverage of the station data which PRISM ingests, causing it to miss some coastal microclimates and weather systems, as well as possibly affecting the accuracy of its regional-scale coastal-proximity interpolation coefficients. Additional refinements in gridded observational products and interpolation methodologies, focusing on carefully evaluating coastlines and their environs, would aid in reducing these issues.

We find that historical coastal cooling reduces instances of daily maxima above 35 °C by an average of nearly 60% within 30 km of the coast, and by 35% with 60 km of the coast, infiltrating far enough inland to affect major portions of the metropolitan areas of Houston, Tampa, Miami, New York City, and Boston. These reductions of 1 °C–4 °C are critical for human health, as mortality rises nonlinearly for daily-maximum temperatures above 35 °C (Gosling *et al* 2007, Wu *et al* 2014). Applying temperature-mortality relationships from Petkova *et al* (2014) for New York City (assuming equivalent dose responses for all regions) yields a rough estimate that observed eastern-US coastal cooling reduces mortality by ∼20%, amounting to around 1000 fewer deaths per year for the historical total annual exposure of 200 million person-days. This calculation omits additional economic savings (such as reduced need for air conditioning). Such coastal-cooling-based reductions in population exposure are much larger than those obtained from downscaled simulations like those we evaluate here, suggesting an important shortcoming of current climate projections along coasts. Our geophysical results are likely invariant to changes in coastlines due to sea-level rise; however, these exposure numbers would almost certainly vary based on future spatial population redistributions, which we do not consider.

The projected intensification in future coastal cooling of ~0.5 °C (figure 3) gives the coastal-cooling effect a continuing importance in mitigating population exposure to extreme heat in a world that is rapidly warming (Jones *et al* 2018). It is also consistent with strong correlations between coastal cooling and land-sea temperature contrast (figure 2) and with the expected circulation response to increases in warm-season land-sea temperature contrast (Dong *et al* 2009, Joshi *et al* 2008). However, such changes derive from a combination of offsetting atmospheric and oceanic responses (Kamae *et al* 2014), meaning that connecting them directly to coastal cooling would require targeted modeling experiments in follow-up work. High-resolution coupled atmosphere-ocean modeling, focusing on coastal atmospheric boundary layers, would be essential to verify and better understand regional differences in present and future coastal cooling. However, the dominant factor for extreme-heat projections along the coast, as elsewhere, is the 3 °C–6 °C average eastern-US summer warming by the late 21st century under RCP8.5 (figure 4(a)) (Lynch *et al* 2016, Vose *et al* 2017). Intermodel agreement about the sign and relative magnitude of these future changes, despite considerable differences over the historical period, is likely due to the downscaling method's preservation of the forced response to global-mean warming (Hall 2014).

We find here that future extreme heat will vary widely over distances that are too small for state-of-the-art global models to properly simulate, even when downscaled. Understanding this variation is valuable in evaluating adaptation strategies and allocating resources for mitigation of impacts, particularly in polities that include both coastal and inland areas. Local fine-scale processes must therefore be considered carefully in order to ensure an accurate assessment of the present and future risks posed by extreme heat along the coastline of the eastern US.

Acknowledgments

Part of this work was carried out at the Jet Propulsion Laboratory, California Institute of Technology, under a contract with the National Aeronautics and Space Administration.

Data availability

The data that support the findings of this study are openly available: PRISM (http://prism.oregonstate.edu, http://doi.org/10.1002/joc.1688), LOCA (http://loca.ucsd.edu, http://doi.org/10.1175/jhm-d-14-0082.1), WRF (http://doi.org/10.1002/2017ef000642), weather stations (https://ncdc.noaa.gov/ghcn-daily-description, http://doi.org/10.1175/jtech-d-11-00103.1), and population density (http://doi.org/10.7927/H4SF2T42).

ORCID iDs

Colin Raymond https://orcid.org/0000-0003-3093-5774
Justin S Mankin https://orcid.org/0000-0003-2520-4555

References

Arritt R W 1993 Effects of the large-scale flow on characteristic features of the sea breeze *J. Appl. Meteorol.* **32** 116–25
Ashfaq M, Rastogi D, Mei R, Kao S-C, Gangrade S, Naz B S and Touma D 2016 High-resolution ensemble projections of near-term regional climate over the continental United States *J. Geophys. Res. Atmos.* **121** 9943–63
Center for International Earth Science Information Network—CIESIN—Columbia University 2016 *Gridded Population of the World, Version 4 (GPWv4): Population Count Adjusted to Match 2015 Revision of UN WPP Country Totals* (Palisades, NY: NASA Socioeconomic Data and Applications Center (SEDAC)) (Accessed: 05 May 2018) (https://doi.org/10.7927/H4SF2T42)
Clemesha R E S, Guirguis K, Gershunov A, Small I J and Tardy A 2018 California heat waves: their spatial evolution, variation, and coastal modulation by low clouds *Clim. Dyn.* **50** 4285–301
Coffel E, Horton R M and de Sherbinin A 2018 Temperature and humidity based projections of a rapid rise in global heat stress exposure during the 21st century *Environ. Res. Lett.* **13** 014001
Coffel E D, Horton R M, Winter J M and Mankin J S 2019 Nonlinear increases in extreme temperatures paradoxically dampen increases in extreme humid-heat *Environ. Res. Lett.* **14** 084003
Daly C, Halbleib M, Smith J I, Gibson W P, Doggett M K, Taylor G H, Curtis J and Pasteris P P 2008 Physiographically sensitive mapping of climatological temperature and precipitation across the conterminous United States *Int. J. Climatol.* **28** 2031–64
Daly C, Helmer E H and Quiñones M 2003 Mapping the climate of Puerto Rico, Vieques, and Culebra *Int. J. Clim.* **23** 1359–81
Diffenbaugh N S, Pal J S, Trapp R J and Giorgi F 2005 Fine-scale processes regulate the response of extreme events to global climate change *Proc. Natl Acad. Sci.* **102** 15774–8
Dong B, Gregory J M and Sutton R T 2009 Understanding land-sea warming contrast in response to increasing greenhouse gases: I. Transient adjustment *J. Clim.* **22** 3079–97
Dunne J P, Stouffer R J and John J G 2013 Reductions in labour capacity from heat stress under climate warming *Nat. Clim. Change* **3** 563–6
Finkele K 1998 Inland and offshore propagation speeds of a sea breeze from simulations and measurements *Bound.-Layer Meteorol.* **87** 307–29
Freychet N, Tett S F B, Hegerl G C and Wang J 2018 Central-Eastern China persistent heat waves: evaluation of the AMIP models *J. Clim.* **31** 3609–24
Gao Y, Fu J S, Drake J B, Liu Y and Lamarque J-F 2012 Projected changes of extreme weather events in the eastern United States based on a high resolution climate modeling system *Environ. Res. Lett.* **7** 044025
Gilliam R C, Raman S and Niyogi D D S 2004 Observational and numerical study on the influence of large-scale flow direction and coastline shape on sea-breeze evolution *Bound.-Layer Meteorol.* **111** 275–300
Gosling S N, McGregor G R and Páldy A 2007 Climate change and heat-related mortality in six cities: I. Model construction and validation *Int. J. Biometeorol.* **51** 525–40
Hall A 2014 Projecting regional change *Science* **346** 1461–2
Horton R M, Mankin J S, Lesk C, Coffel E and Raymond C 2016 A review of recent advances in research on extreme heat events *Curr. Clim. Change Rep.* **2** 242–59

Hu X-M and Xue M 2016 Influence of synoptic sea-breeze fronts on the urban heat island intensity in Dallas-Fort Worth, Texas *Mon. Weather Rev.* **144** 1487–507
Jones B, O'Neill B C, McDaniel L, McGinnis S, Mearns L O and Tebaldi C 2015 Future population exposure to US heat extremes *Nat. Clim. Change* **5** 652–5
Jones B, Tebaldi C, O'Neill B C, Oleson K and Gao J 2018 Avoiding population exposure to heat-related extremes: demographic change vs climate change *Clim. Change* **146** 423–37
Joshi M M, Gregory J M, Webb M J, Sexton D M H and Johns T C 2008 Mechanisms for the land/sea warming contrast exhibited by simulations of climate change *Clim. Dyn.* **30** 455–65
Kamae Y, Watanabe M, Kimoto M and Shiogama H 2014 Summertime land-sea thermal contrast and atmospheric circulation over East Asia in a warming climate: II. Importance of CO_2-induced continental warming *Clim. Dyn.* **43** 2569–83
Kunreuther H, Heal G, Allen M, Edenhofer O, Field C B and Yohe G 2013 Risk management and climate change *Nat. Clim. Change* **3** 447–51
Lebassi B, Gonzalez J, Fabris D, Maurer E, Miller N, Milesi C, Switzer P and Bornstein R 2009 Observed 1970–2005 cooling of summer daytime temperatures in coastal California *J. Clim.* **22** 3558–73
Lebassi-Habtezion B, Gonzalez J and Bornstein R 2011 Modeled large-scale warming impacts on summer California coastal-cooling trends *J. Geophys. Res.* **116** D20114
Li G, Zhang X, Zwiers F and Wen Q H 2012 Quantification of uncertainty in high-resolution temperature scenarios for North America *J. Clim.* **25** 3373–89
Liang X-Z, Pan J, Zhu J, Kunkel K E, Wang J X L and Dai A 2006 Regional climate model downscaling of the US summer climate and future change *J. Geophys. Res.* **111** D10108
Lynch C, Seth A and Thibeault J 2016 Recent and projected annual cycles of temperature and precipitation in the Northeast United States from CMIP5 *J. Clim.* **29** 347–65
Maraun D *et al* 2017 Towards process-informed bias correction of climate change simulations *Nat. Clim. Change* **7** 764–73
Meinshausen M *et al* 2011 The RCP greenhouse gas concentrations and their extensions from 1765 to 2300 *Clim. Change* **109** 213–41
Meir T, Orton P M, Pullen J, Holt T, Thompson W T and Arend M F 2013 Forecasting the New York City urban heat island and sea breeze during extreme heat events *Weather Forecast.* **28** 1460–77
Melecio-Vázquez D, Ramamurthy P, Arend M and González-Cruz J E 2018 Thermal structure of a coastal-urban boundary layer *Bound.-Layer Meteorol.* **169** 151–61
Menne M J, Durre I, Vose R S, Gleason B E and Houston T G 2012 An overview of the global historical climatology network-daily database *J. Atmos. Ocean. Technol.* **29** 897–910
Miller N L, Hayhoe K, Jin J and Auffhammer M 2008 Climate, extreme heat, and electricity demand in California *J. Appl. Meteorol. Climatol.* **47** 1834–44
Misra V, Moeller L, Stefanova L, Chan S, O'Brien J J, Smith T J III and Plant N 2011 The influence of the Atlantic Warm Pool on the Florida panhandle sea breeze *J. Geophys. Res.* **116** D00Q06
Mora C *et al* 2017 Global risk of deadly heat *Nat. Clim. Change* **7** 501–6
Ning L, Riddle E E and Bradley R S 2015 Projected changes in climate extremes over the northeastern United States *J. Clim.* **28** 3289–310
Novak D R and Colle B A 2006 Observations of multiple sea breeze boundaries during an unseasonably warm day in metropolitan New York City *Bull. Am. Meteorol. Soc.* **87** 169–74
Papalexiou S M, AghaKouchak A, Trenberth K E and Foufoula-Georgiou E 2018 Global, regional, and megacity trends in the highest temperature of the year: diagnostics and evidence for accelerating trends *Earth's Future* **6** 71–9
Petkova E P, Gasparrini A and Kinney P L 2014 Heat and mortality in New York City since the beginning of the 20th century *Epidemiology* **25** 554–60
Pierce D W, Cayan D R, Maurer E P, Abatzoglou J T and Hegewisch K C 2015 Improved bias correction techniques for hydrological simulations of climate change *J. Hydrometeorol.* **16** 2421–42
Pierce D W, Cayan D R and Thrasher B L 2014 Statistical downscaling using localized constructed analogs (LOCA) *J. Hydrometeorol.* **15** 2558–85
Sequera P, Gonzalez J E, McDonald K, Bornstein R and Comarazamy D 2015 Combined impacts of land cover changes and large-scale forcing on Southern California summer daily maximum temperatures *J. Geophys. Res. Atmos.* **120** 9208–19
Smith T T, Zaitchik B F and Gohlke J M 2013 Heat waves in the United States: definitions, patterns, and trends *Clim. Change* **118** 811–25
Thibeault J M and Seth A 2014 Changing climate extremes in the Northeast United States: observations and projections from CMIP5 *Clim. Change* **127** 273–87
Vose R S, Easterling D R, Kunkel K E, LeGrande A N and Wehner M F 2017 Temperature changes in the United States *Climate Science Special Report: Fourth National Climate Assessment* ed D J Wuebbles *et al* (Washington, DC: US Global Change Research Program) vol I, pp 185–206
Wang J and Kotamarthi V R 2014 Downscaling with a nested regional climate model in near-surface fields over the contiguous United States *J. Geophys. Res. Atmos.* **119** 8778–97
Wilson S G and Fischetti T R 2010 Coastline population trends in the United States: 1960 to 2008 *US Census Bureau, Population Division, Report* P25–1139 (Suitland, MD: US Census Bureau)
Wu J, Zhou Y, Gao Y, Fu J S, Johnson B A, Huang C, Kim Y-M and Liu Y 2014 Estimation and uncertainty analysis of impacts of future heat waves on mortality in the eastern United States *Environ. Health Perspect.* **122** 10–6
Wuebbles D *et al* 2015 CMIP5 climate model analyses: climate extremes in the United States *Bull. Am. Meteorol. Soc.* **95** 571–83
Xie S-P *et al* 2015 Towards predictive understanding of regional climate change *Nat. Clim. Change* **5** 921–30
Zhang B and Soden B J 2019 Constraining climate model projections of regional precipitation change *Geophys. Res. Lett.* **46**
Zhao Z, Chen S-H, Kleeman M J and Mahmud A 2011 The impact of climate change on air quality-related meteorological conditions in California: II. Present versus future time simulation analysis *J. Clim.* **24** 3362–76
Zobel Z, Wang J, Wuebbles D J and Kotamarthi V R 2017 High-resolution dynamical downscaling ensemble projections of future extreme temperature distributions for the United States *Earth's Future* **5** 1234–51
Zobel Z, Wang J, Wuebbles D J and Kotamarthi V R 2018 Evaluations of high-resolution dynamically downscaled ensembles over the contiguous United States *Clim. Dyn.* **50** 863–84